Vol 17 No 12, December 2008
1674-1056/2008/17(12)/4562-06

Chinese Physics B

© 2008 Chin. Phys. Soc.
and IOP Publishing Ltd

Analysis of $D_\alpha(H_\alpha)$ spectrum emitted in front of the limiter in HT–7*

Huang Juan(黄 娟)[a)†], Wan Bao-Nian (万宝年)[a)], Daren Stotler[b)],
Xiao Bing-Jia(肖炳甲)[a)], Wu Zhen-Wei(吴振伟)[a)], and the HT–7 team[a)]

[a)] *Institute of Plasma Physics, Chinese Academy of Sciences, P.O. Box 1126, Hefei* 230031, *China*

[b)] *Princeton Plasma Physics Laboratory, Princeton University, Princeton, New Jersey* 08543, *USA*

(Received 27 May 2008; revised manuscript received 25 June 2008)

In order to understand the recycling and emission processes of hydrogen atoms in HT–7, spectral profiles of the $D_\alpha(H_\alpha)$ line emitted in front of the limiter have been observed with a high-resolution spectrometer and simulated by using the neutral particle transport code DEGAS 2. The results show that four processes are necessary to interpret the $D_\alpha(H_\alpha)$ line shape: 1) atom desorption, 2) molecular dissociation, 3) particle reflection, and 4) charge-exchange. The products of the first two processes are cold atoms which emit photons near the peak of $D_\alpha(H_\alpha)$ line shape, and those from the last two are warm atoms contributing to the blue side of the spectrum. For a typical ohmic discharge (shot 68520 $n_e(0) \approx 3 \times 10^{19}\,m^{-3}$), these components contribute 32%, 15%, 32% and 21%, respectively. $D_\alpha(H_\alpha)$ line shapes under different plasma parameters are also discussed in this paper.

Keywords: tokamak, edge recycling, $D_\alpha(H_\alpha)$ line shape
PACC: 5220, 5240

1. Introduction

For extrapolation to future fusion reactor devices, an understanding of the edge plasma in present tokamaks is necessary. The transport of neutrals, atomic processes, and plasma-wall interactions play key roles in edge plasma physics. To study basic recycling processes,[1] the spectral profile of the D_α line emitted from the divertor region of JT-60U was measured and simulated. In TFTR, Monte Carlo neutral transport simulations of hydrogen velocities using DEGAS were compared with measurements using Balmer-α spectral line profile.[2] In TEXTOR, the profiles of the $D_\alpha(H_\alpha)$ lines emitted in front of limiters were observed with high-resolution spectrometers and analysed by Monte Carlo calculations.[3] H_α line shape was once analysed by multi-Gaussian fitting[4] in front of the limiter in the HT-6M. The spectral profile of the H_α line contains abundant information on the velocity distribution of hydrogen atoms which determines their penetration depth into plasmas and their basic recycling processes. Understanding the behaviour of hydrogen atoms in the edge region is necessary to control fuelling and pumping in fusion plasmas.

For the HT–7 tokamak of a limiter configuration, recycling particles contribute more than 90% of the total fuelling to sustain particle balance during the plateau of a discharge.[5] The limiter plays an important role in edge recycling, so the study of recycling from the limiter is the focus of this paper. To investigate the recycling mechanism in detail, the $D_\alpha(H_\alpha)$ line shape was simulated by using DEGAS 2.[6] In order to further clarify observations and understand recycling processes, the $D_\alpha(H_\alpha)$ line shape is obtained and simulated under different plasma parameters and will be discussed in this paper.

The rest of the paper is organized as follows. In Section 2, a description of relevant diagnostics is given. A brief description of DEGAS 2 code and the simulation method for HT–7 are presented in Section 3. In Section 4, the basic recycling processes of deuterium atoms are discussed by comparing the observations and the simulations of the $D_\alpha(H_\alpha)$ spectral profile under different plasma parameters. Finally, a short summary is given in Section 5.

2. Experimental measurement

HT–7 is a medium-sized iron core superconducting tokamak. The main parameters are major radius

*Project supported by the National Natural Science Foundation of China (Grant No 10725523).
†Corresponding author. E-mail: janejoy@ipp.ac.cn

$R = 1.22\,\mathrm{m}$; minor radius $a = 0.27\,\mathrm{m}$; the working gas is deuterium. It is equipped with active water-cooled up-down symmetric toroidal limiters and belt limiters located on the high-field side as shown in Fig.1. A new form of doped graphite with a SiC gradient coating is chosen as the plasma facing material. Edge electron density and temperature profiles from 25 to 30 cm in radius are measured by using a Langmuir probe located on the top of the tokamak along the central line.[7] Plasma electron density profile from 0 to 25 cm in radius is measured by using a vertical 5-channel far-infrared hydrogen cyanide (HCN) laser interferometer.[8] The electron temperature profile is estimated from the soft x-ray pulse height analyser (PHA).[9] The central ion temperature is measured with the neutral particle analyser (NPA).[10]

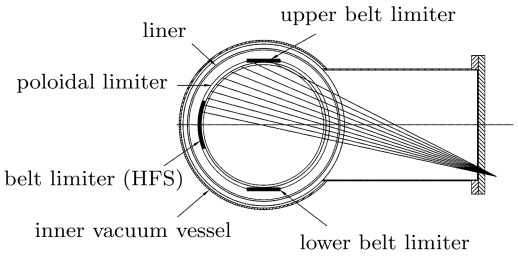


Fig.1. Schematic diagram in the poloidal cross-section of HT–7 tokamak.

The $D_\alpha(H_\alpha)$ spectral profile is measured by using an optical multi-channel analysis (OMA) system. It is equipped with a high-resolution Acton Research Spectrometer (SP-750) and ICCD (EEV 384×578 pixels) cooled by a multistage Peltier element. The 2400 gr/mm grating is used with a spectral resolution of 0.01 nm. Ten lines of sight shown in Fig.1 go through the upper-midplane plasma region. The lowest chord of these sights, used for this analysis, passes through the plasma centre facing the belt limiter located on the high field side. Thus, the photons from particles moving towards the centre are Doppler shifted to shorter wavelengths, and wavelength shift due to plasma rotation is avoided. The measured $D_\alpha(H_\alpha)$ line shape is determined by the convolution of a number of effects: the instrument function, the geometry of observation, the geometry of the source, the effects of plasma profiles, atomic and molecular processes, etc. Because of the strong toroidal magnetic field perpendicular to the plane of observation, the $D_\alpha(H_\alpha)$ spectral line is split into three Zeeman components. The two σ components can be eliminated by the use of a suitably orientated polarizer, and the measurements refer to the unshifted single π component. The instrument function is taken as the measured shape of 6328Å (1 Å = 0.1 nm) He-Ne laser line and can be deconvolved. Corresponding to the 2400 gr/mm grating with a slit width of 50 μm, the measured instrumental width is about 0.03 nm with Gaussian profile. Electric fields in the plasma also affect the energy level structure of hydrogenic ions through the Stark effect; however, the ambipolar fields and ion microfields are generally too small to influence spectral line widths. So, the Doppler Effect is dominant.

3. Simulation

In this work, the simulation of $D_\alpha(H_\alpha)$ line shape is performed by using the three-dimensional neutral gas transport code DEGAS 2 in which toroidal symmetry is assumed. For a given geometry and plasma parameters, neutral atoms and molecules are tracked by using the Monte Carlo technique as they undergo ionization, charge exchange, dissociation, and interactions with surfaces. The result is effectively a numerical solution of the Boltzmann equation for a neutral distribution function.

As shown in Fig.1, the magnetic geometry of HT–7 is assumed to be a circular configuration. According to the characteristics of tokamak plasma parameters and magnetic geometry, four regions are set: core plasma (0–25 cm), cold plasma (25–27 cm), scrape-off-layer (SOL) plasma (27–30 cm), and vacuum (30–33 cm).

In the simulation, it is assumed that the hydrogen ions arriving at the limiter are either reflected as atoms or desorbed as atoms and molecules. The H^+ flux or current to the surface is input to DEGAS 2. In computing the neutral profile associated with that source, DEGAS 2 begins by sampling an ion from that flux through using the ion temperature and velocity near that surface. The local sheath potential is evaluated by using the electron temperature there and accelerates the ion to the target. This gives the energy with which the ion will strike the plate. It is assumed that it hits at normal incidence. The ion is assumed to be neutralized by the cloud of electrons at the surface, and thus it interacts with the material as an atom. This allows us to use the same set

of particle-material interactions to describe incoming ions and atoms. Some neutralized ions are reflected as atoms (H + C → H shown label K in Table 1). The reflected atoms originating from the ion incident on the limiter have the energies $E_{\rm refl} = R_{\rm E}(E_{\rm i} + \Phi_{\rm sh})$, where $R_{\rm E}$ is the fraction of the incident energy retained by the reflected atoms, which is dependent on the incident angle, energy and the target material, $E_{\rm i}$ is the ion energy before the sheath, $\Phi_{\rm sh}$ is the sheath potential, which is taken as $3T_{\rm e}$. The dependences of reflection yield and energy reflection coefficient on the incident energy used are from 'refl.dat' in DEGAS 2 which is calculated by using VFTRIM code.[11] Reflected particles are assumed to have a cosine angular distribution. In low incident energies of carbon or deuterium, the sputtering yield of deuterium is less than the reflection yield.[2] So, in our case the sputtering of hydrogen isotopes from the graphite limiter can be neglected. Deuterium ions that are not reflected are assumed to be desorbed as atoms or molecules with an energy of the surface temperature of the limiter. In Ref.[12], it was observed that at the limiter temperature $T_{\rm TL} \geq 1100\,{\rm K}$ the direct atomic release was dominant, whereas at low temperatures ($550\,{\rm K} < T_{\rm TL} < 1100\,{\rm K}$) the ratio of molecules to atoms is unknown. Thus, desorption process is set as H + C→H+ H_2 (label L in Table 1). Molecular hydrogen entering the plasma will be ionized and/or dissociated by electron collisions. Table 1 lists all atomic and molecular reactions considered in our simulation. The energy of the hydrogen product atoms depends on the particular dissociation pathway and the energy transferred from the electron.[8]

Table 1. Atomic and molecular processes considered in DEGAS 2 (A—J); Plasma and surface interactions (K: reflection, L: desorption).

Label	Processes
A	H_2+e→H(1s)+H(1s)+e
B	H_2+e→H*(n = 3)+H(1s)+e
C	H_2+e→ e+H_2^++e
D	H_2+e→H(1s)+H^++ e
E	H_2^++e→ e + H^+ + H^+ + e
F	H_2^++e→ H(1s)+ H^++e
G	H_2^++e→ H*(n = 3)+H^+ +e
H	H_2^++e→ H*(n = 3)+H(1s)
I	H + e → e+H^++e
J	H+H^+ → H^++H
K	H + C → H(Reflection)
L	H + C → H + H_2(Desorption)

4. Results and discussion

The electron density $n_{\rm e}$ and the electron (ion) temperature $T_{\rm e}(T_{\rm i})$ of a typical ohmic discharge 68520 are shown in Figs.2 and 3, respectively, which are fitting chart according to repetitively measured raw data. The ion temperature profiles are not available and treated as an adjustable parameter. Owing to the charge exchange process and particle reflection, it mainly influences the blue side of the spectrum. The higher the ion temperature is, the broader the far wing component will be.

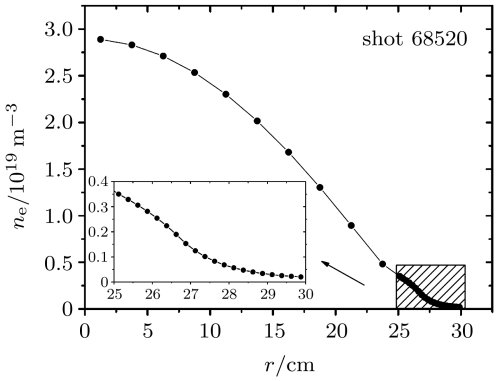


Fig.2. Radial distribution of electron density $n_{\rm e}(r)$ for ohmic discharge shot 68520.

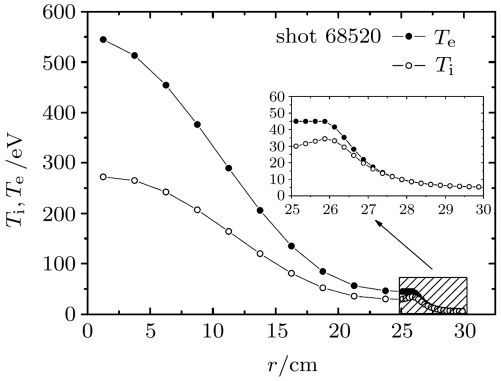


Fig.3. Radial distribution of electron and ion temperatures (shot 68520).

The spectral profiles for the present study are measured in the plateau state of this discharge with an integration time of 0.1 s. Figure 4 shows the observed $D_\alpha(H_\alpha)$ line shape and the $H_\alpha$spectral profile from a hydrogen lamp for a comparison. The working gas is deuterium; hydrogen comes from the wall and limiter surfaces. The rest wavelength of $H_\alpha$is 656.285 nm (D_α: 656.104 nm), and the central wavelengths of observed D_α and H_α line shape are 656.102 and 656.276 nm, respectively. It is shown that compared with standard H_α shape, the spectrum differs strongly from

the Gaussian profile and is clearly asymmetric with a slight but significant blue shift of the peak.

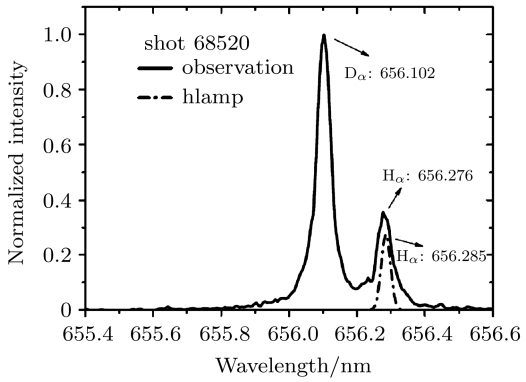


Fig.4. The observed $D_\alpha(H_\alpha)$ spectrum (solid line) in a typical ohmic discharge (shot 68520) and H_α line shape (dashed) from a hydrogen lamp.

Observed and simulated $D_\alpha(H_\alpha)$ spectra are shown in Fig.5. The simulated line profile accords reasonably well with that observed. The isotopic mix of incident hydrogen ions is adjusted to match that experimentally observed in the Balmer-α spectral profile. According to the area of the shape of the $D_\alpha(H_\alpha)$ spectra, the ratio of H/(H+D) is about 30%.

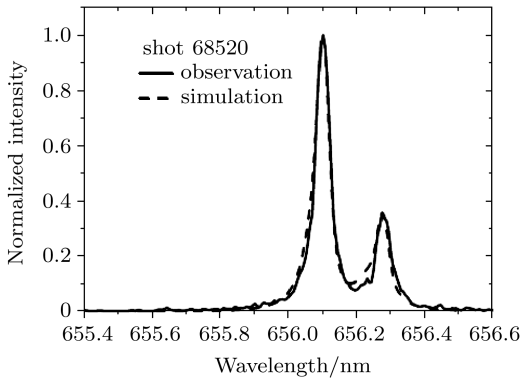


Fig.5. Observed (solid line) and simulated (dashed) $D_\alpha(H_\alpha)$ spectra of shot 68520.

Figure 6 shows that four processes are necessary to interpret $D_\alpha(H_\alpha)$ line shape: 1) atom desorption, 2) molecular reactions, 3) particle reflection, and 4) charge-exchange. The products from the first two processes are cold atoms which emit photons near the peak $D_\alpha(H_\alpha)$ line shape, and those from the last two are warm atoms contributing to the blue side of the spectrum. These components have the proportions 32%, 15%, 32% and 21%, respectively. Atom desorption and reflection are the two dominant processes in edge recycling. Although the charge-exchange does not contribute to particle recycling directly, it can transfer energy from plasma ions to atoms produced by dissociated, increasing their penetration into the plasma.

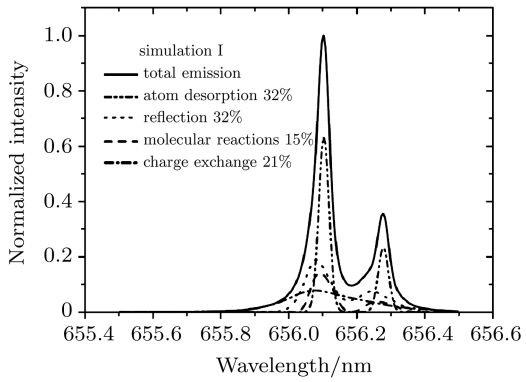


Fig.6. Proportions of the simulated $D_\alpha(H_\alpha)$ spectrum in four processes: 1) atom desorption (32%), 2) molecular reaction (15%), 3) particle reflection (32%), 4) charge-exchange reaction (21%).

Since the edge density is insufficient to thermalize the velocity distribution, the contributions of the various reaction pathways that generate hydrogen atoms may be associated with different wavelength regions (velocities) in the spectral profile. For atom desorption, the position of its simulated peak is at 656.102 nm. According to Doppler shift, a mean energy of an atom is about 0.05 eV which corresponds to 600 K of the limiter temperature. The limiter temperature used in DEGAS 2 is based on measurements. This leads to a slight shift in the peak of the emission from desorbed atoms, which seems consistent with observations. The peak of the reflection component is 656.082 nm, corresponding to an energy of 12 eV. The models used in the code imply a shift in the emission from reflected atoms. The resulting emissions are consistent with observations, showing the overall agreement between the observed and the simulated spectra. Those atoms from molecular reactions have a mean energy of 3.7 eV. The detailed compositions of the molecular reactions are shown in Fig.7. There are two principal breakup reactions, i.e. dissociation into two ground state atoms (A in Table 1) and ionization (C in Table 1) followed by dissociation (F in Table 1). In molecular reactions, F contributes 42% to Balmer-α emission, and A about 21%. The edge electron temperature of this shot from 25–27 cm is about 40–15 eV shown in Fig.3. Under these conditions, molecular ion dissociation and molecular ionization are the two principal breakup reactions.

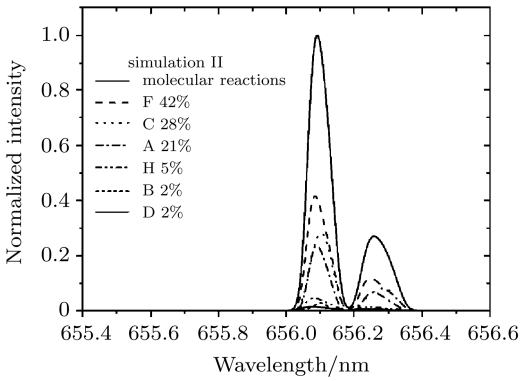


Fig.7. Detailed proportions of the molecular reaction component (each label is shown in Table 1).

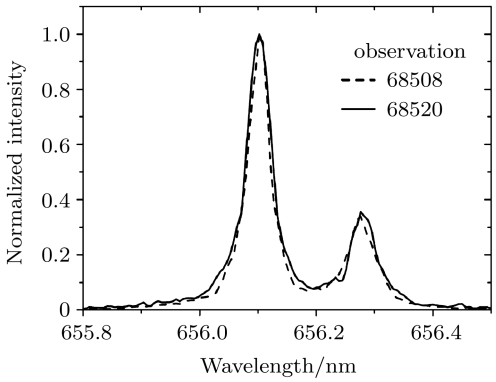


Fig.8. Comparison between $D_\alpha(H_\alpha)$ observed spectra in shots 68508 and 68520.

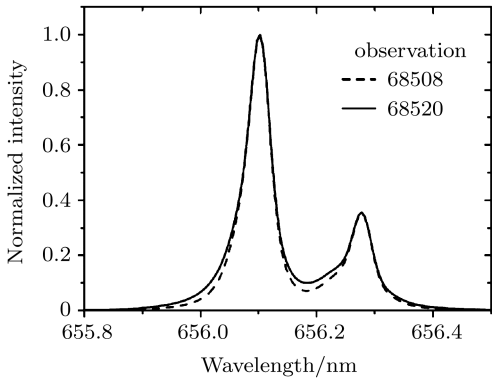


Fig.9. Comparison between $D_\alpha(H_\alpha)$ simulated spectra in shots 68508 and 68520.

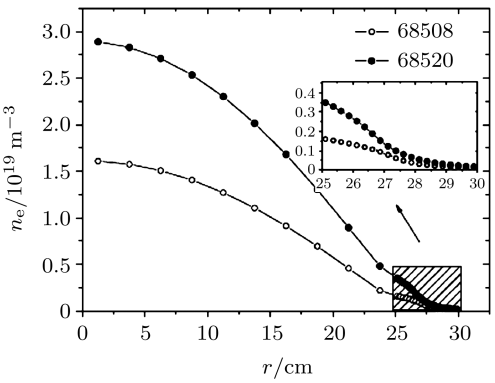


Fig.10. Radial distributions of electron density $n_e(r)$ for shots 68520 and 68508.

To understand the phenomena observed in the $D_\alpha(H_\alpha)$ line shape, the characteristics of edge plasma must be examined more closely. The deuterium ionization length can be expressed as $\lambda_i = v_D/(n_e\langle\sigma v_i\rangle)$. The reaction rates for the most important neutral processes are given in Ref.[13]. As can be seen in Ref.[1] for temperatures lower than 15 eV, Franck–Condon (F-C) breakup of D_2 into atoms is important, while above 15 eV, direct ionization dominates. In a typical HT–7 ohmic discharge plasma, edge parameters are $n_e(a) \approx 2\times10^{18}\mathrm{m}^{-3}$ and $T_e(a) \approx 20$eV. First, for thermal D_2 particles, $v_D \approx 1.7\times10^5$ cm/s, and $\langle\sigma v_i\rangle \approx 2\times10^{-8}$ cm^3/s, then $\lambda_i \approx 4$cm, which shows that recycling molecules can exist only near the limiter region. Secondly, D_2 ionization by electron impact predominates, producing F-C atoms with an average energy of 4.3 eV corresponding to $v_D \approx 2\times10^6$ cm/s, $\langle\sigma v_i\rangle \approx 1.5\times10^{-8}$ cm^3/s, and $\lambda_i \approx 60$ cm. Thus, not only charge-exchange atoms but also FC atoms can reach the core plasma. During ionization, ion molecules D_2^+ can also be formed, $v_D \approx 1\times10^5$ cm/s, $\langle\sigma v_i\rangle \approx 2\times10^{-7}$ cm^3/s, $\lambda_i \approx 0.25$ cm, that means once D_2^+ is formed, it will be dissociated immediately.

Comparisons between observed $D_\alpha(H_\alpha)$ spectra and between the simulated ones in shots 68508 and 68520 are shown in Figs.8 and 9 respectively. The radial plasma electron density profile $n_e(r)$ and electron temperature profile $T_e(r)$ of low-density shot 68508 ($n_e(0) \approx 1.5\times10^{19}$ m^{-3}) and a high-density shot 68520 ($n_e(0) \approx 3\times10^{19}$ m^{-3}) are given in Figs.10 and 11. These show that when the electron density decreases, the edge electron temperature increases.

The $D_\alpha(H_\alpha)$ line shape in the high-density case is slightly broader than that of the low-density case in Fig.8. The simulated spectra match the observations well, and the comparison between the simulated ones exhibits the same trend. Figure 12 shows the composition of the simulated $D_\alpha(H_\alpha)$ spectrum. The possible reason for the narrower spectrum in the low density case is that an increase in electron temperature enhances a proportion of atom desorption component to 38%, making the peak component seem narrower. In JT-60U,[1] this phenomenon was also observed and explained as follows: as the electron temperature decreased in high-density cases, the contribution of dissociative recombination became important. But in our

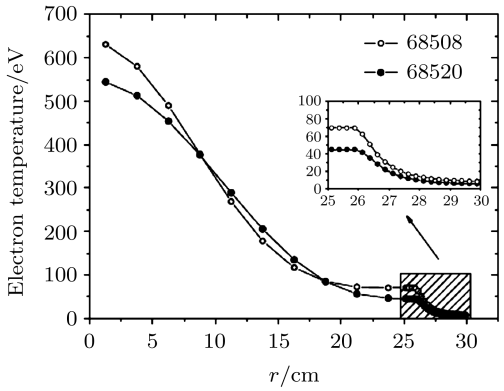


Fig.11. Radial distribution of electron temperature for shot 68520 and 68508.

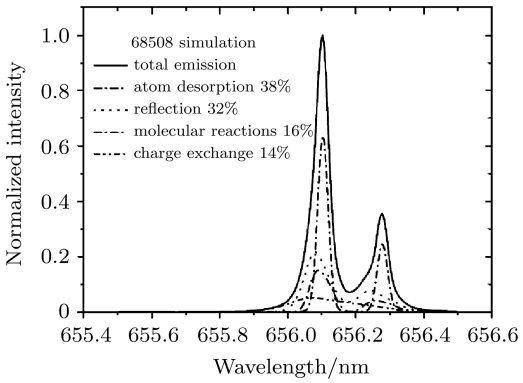


Fig.12. Composition of the simulated $D_\alpha(H_\alpha)$ spectrum.

case, dissociative recombination component is less than 5% and can be neglected. It may be due to the different configurations. For JT-60U, it was observed in front of the divertor tile in which the neutral density was high, making recombination more important. The wings of the profile in Fig.8 are also narrower in the low-density case. The lower collision frequency between electrons and ions in this case can reduce the ion temperature, so that the energies of atoms from reflection and charge-exchange reaction are lower, making distribution narrower.

5. Summary

To investigate the recycling mechanism in HT–7, spectral profiles of $D_\alpha(H_\alpha)$ emitted from the limiter have been observed and simulated. The results show that four processes are necessary to interpret the $D_\alpha(H_\alpha)$ line shape: 1) atom desorption, 2) molecular dissociation, 3) particle reflection, and 4) charge-exchange. For a typical ohmic discharge shot 68520 ($n_e(0) \approx 3 \times 10^{19}\,m^{-3}$), these components have the proportions 32%, 15%, 32% and 21%, respectively. Atom desorption and particle reflection are the two dominant processes in edge recycling. In high-density cases, the narrow component of the $D_\alpha(H_\alpha)$ spectrum is clearly broader than that in low-density cases. It is because when the electron density increases, the electron temperature decreases, which may reduce atom desorption component. To understand recycling mechanism in detail for HT–7, more work should be done. Spatial distribution of the $D_\alpha(H_\alpha)$ spectrum and its evolution during a long pulse discharge should be investigated and simulated further.

Acknowledgments

We are grateful to the HT–7 operation and diagnostics teams.

References

[1] Kubo H, Takenaga H, Sugie T, Higashijima S, Suzuki S, Sakasai A and Hosogane N 1998 *Plasma Phys. Control. Fusion* **40** 1115

[2] Stotler D P, Skinner C H, Budny R V, Ramsey A T, Ruzic D N and Turkot Jr R B 1996 *Phys. Plasmas* **3** 4084

[3] Samm U, Bogen P, Hartwig H, Hintz E, Hothker K, Lie Y T, Pospieszczyk A, Rusbüldt D, Schweer B and Yu Y J 1989 *J. Nucl. Mater.* **162-164** 24

[4] Wan B N, Li J G, Luo J R, Xie J K, Wu Z W, Zhang X M and HT-6M Group 1999 *Nucl. Fusion* **39** 1865

[5] Huang J, Wan B N, Li J G, Gong X Z, Zhang X D, Wu Z W, Zhou Q and HT–7 team 2006 *Nucl. Fusion* **46** 262

[6] Stotler D P and Karney C F 1994 *Contrib. Plasma Phys.* **34** 392

[7] Xu G S, Song M, Wan B N, Ling B L, Li C F, Li J and HT–7 Team 2003 *J. Nucl. Mater* **313-316** 259

[8] Jie Y X, Gao X, Cheng Y F, Yang K and Tong X D 2000 *Plasma Sci. Technol.* **2** 105

[9] Shi Y J, Chen Z Y, Wan B N, Lv B, Hu L Q, Lin S Y, Hu Q S, Qian J P, Liu H Q, Liu S X, Xu Y C, Shan J F and Li J G 2004 *Rev. Sci. Instrum* **75** 4930

[10] Sheng X L, Qin P J, Zhang X M, Wan B N and HT–7 team 2002 *Fusion Eng. Des.* **60** 211

[11] David N Ruzic 1990 *Nucl. Instrum. Methods Phys. Res.* B **47** 118

[12] Brezinsek S, Sergienko G, Pospieszczyk A, Mertens Ph, Samm U and Greenland P T 2005 *Plasma Phys. Control. Fusion* **47** 615

[13] Janev R K, Langer W D, Post D E Jr and Evans Kenneth Jr 1987 *Springer Series on Atoms and Plasmas* **4** (Berlin: Springer)